

Zeitschrift: IABSE publications = Mémoires AIPC = IVBH Abhandlungen
Band: 31 (1971)

Artikel: Variable amplitude fatigue studies on steel beams
Autor: Heins, Conrad P. / Murad, Francis A.
DOI: <https://doi.org/10.5169/seals-24219>

Nutzungsbedingungen

Die ETH-Bibliothek ist die Anbieterin der digitalisierten Zeitschriften. Sie besitzt keine Urheberrechte an den Zeitschriften und ist nicht verantwortlich für deren Inhalte. Die Rechte liegen in der Regel bei den Herausgebern beziehungsweise den externen Rechteinhabern. [Siehe Rechtliche Hinweise.](#)

Conditions d'utilisation

L'ETH Library est le fournisseur des revues numérisées. Elle ne détient aucun droit d'auteur sur les revues et n'est pas responsable de leur contenu. En règle générale, les droits sont détenus par les éditeurs ou les détenteurs de droits externes. [Voir Informations légales.](#)

Terms of use

The ETH Library is the provider of the digitised journals. It does not own any copyrights to the journals and is not responsible for their content. The rights usually lie with the publishers or the external rights holders. [See Legal notice.](#)

Download PDF: 25.05.2025

ETH-Bibliothek Zürich, E-Periodica, <https://www.e-periodica.ch>

Variable Amplitude Fatigue Studies on Steel Beams

Essai de fatigue sur des poutres métalliques sous l'effet d'amplitudes variables

Ermüdungsversuche an Stahlträgern mit variabler Amplitude

CONRAD P. HEINS

Associate Professor, Civil Engineering
Department, University of Maryland,
College Park, Md., U.S.A.

FRANCIS A. MURAD

Research Graduate Assistant, Civil Engineering Department, University of Maryland, College Park, Md., U.S.A.

Introduction

An extensive research program has been initiated in the United States, to obtain field loading history data and the resulting effects on bridge structures [1], [2], [3], [4].

The collection of these data [5], [6], [7], [8] will then permit simulated laboratory studies on various bridge elements.

It is the purpose of this paper to present the results of such a laboratory study, and a proposed fatigue damage hypothesis which considers random loadings. The theory and experiments will only consider steel beams with welded cover plates.

Theory

The fatigue life of a specimen, subjected to stress cycles at varying amplitudes, requires a damage index. Crack growth data might be considered as such an index. However, the difficulty in measuring this phenomenon is difficult if not impossible. An alternate index, which is measurable, is the accumulated plastic strain, which will be utilized in this study.

Stress-Cycle Criteria. Examination of crack growth data [1], [10] indicates that the growth rate is exponential with respect to cycles. Assuming strain accumulation and crack growth behave similarly, the following Eq. (1) is proposed:

$$\frac{d\epsilon_p}{dn} = A \alpha \sigma_r^\gamma n^{\alpha-1}, \quad (1)$$

where A , α and γ are stress dependent material constants, which are to be determined experimentally. The term σ_r represents the stress range which was demonstrated (11) to be the significant parameter in fatigue of steel beams with cover plates.

The total plastic strain at n cycles is:

$$\epsilon_p = A \sigma_r^\gamma n^\alpha \quad (2)$$

and at failure N_f is:

$$\epsilon_f = A \sigma_r^\gamma N_f^\alpha. \quad (3)$$

Eq. (3) can be described in logarithm form as follows, thus representing a typical $\sigma_r - N_f$ diagram.

$$\text{Log } N_f = \frac{1}{\alpha} \text{Log} \left(\frac{\epsilon_f}{A} \right) - \frac{\gamma}{\alpha} \text{Log } \sigma_r \quad (4)$$

or

$$\text{Log } N_f = b - c \text{Log } \sigma_r \quad (5)$$

where:

$$b = \frac{1}{\alpha} \text{Log} \left(\frac{\epsilon_f}{A} \right), \quad c = \frac{\gamma}{\alpha}.$$

Damage Criteria. The rate of damage, as indicated previously, will be reflected on the amount of accumulated strain, or

$$D = \left(\frac{\epsilon_p}{\epsilon_f} \right). \quad (6)$$

Substituting Eqs. (2) and (3) into (6) gives:

$$D = \left(\frac{n}{N_f} \right)^\alpha, \quad (7)$$

where α is a function of the stress range (σ_r), and at failure the value of D will equal one.

Required Coefficients. In order to apply Eqs. (5) and (7), particular coefficients are required. The coefficients b and c of Eq. (5) can be obtained from constant amplitude tests and represent the intercept and slope of a curve of the diagram.

The variable α can be established by obtaining the strain accumulation per cycle $\left(\frac{d\epsilon}{dn} \right)$ Eq. (1) and plotting these data on Log-Log paper vs. n , for the respective stress ranges. This will yield an equation of the form:

$$\text{Log} (\alpha - 1) = d - e \text{Log } \sigma_r, \quad (8)$$

where d and e are constants to be determined experimentally.

Variable Amplitude Analysis. In order to apply the above equations, the damage accumulation process is assumed to be interaction-free. That is, the application of other stress amplitudes will not alter the damage curves established from constant amplitude data. This can be illustrated by examining Fig. 1, where three specimens accumulate damage equal to (D) , resulting from

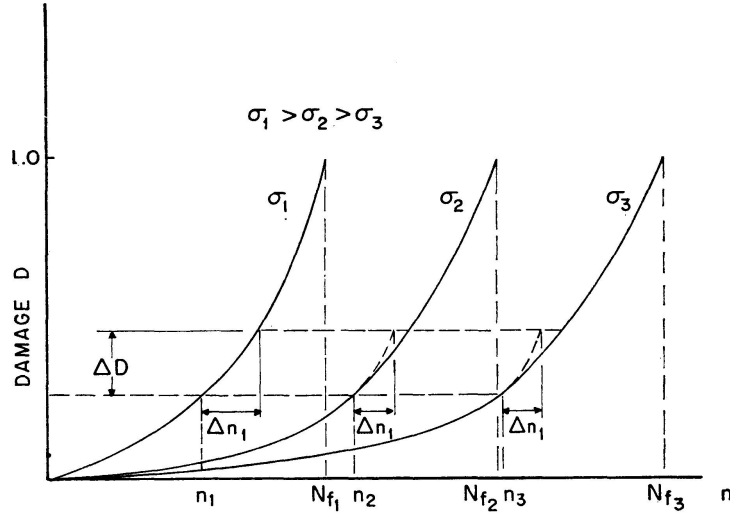


Fig. 1. Hypothetical Damage-Cycle Relationship.

application of stresses and cycles of (σ_1, n_1) ; (σ_2, n_2) ; and (σ_3, n_3) . If the application of an additional (Δn_1) cycle at stress range (σ_1) occurs to any of the specimens, an increment of damage equal to (ΔD) results. The path of the damage curves for all three specimens will be the same as that for specimens loaded at (σ_1) range, and is shown dotted in Fig. 1.

Because the three specimens have equivalent damage, an expression relating the effective cycles at one level (i) to another level $(i+1)$ is formulated as follows:

$$D_i = D_{i+1}$$

and from Eq. (7):

$$\left(\frac{n_i}{N_{fi}}\right)^{\alpha_i} = \left(\frac{n_{i+1}}{N_{fi+1}}\right)^{\alpha_{i+1}}, \quad (9)$$

$$n_{i+1} = N_{fi+1} \left(\frac{n_i}{N_{fi}}\right)^{\alpha_i/\alpha_{i+1}}. \quad (10)$$

With the basic Eqs. (5), (7), (8) and (10) established, the analysis of members subjected to variable amplitude loads can be performed.

Example. Consider a member subjected to (σ_1, n_1) and (σ_2, n_2) stresses and cycles. It is required to determine the number of cycles (n_3) at stress range (σ_3) to cause failure. Fig. 2 describes the loading pattern.

The following will outline the required calculations, with the results presented graphically in Fig. 3.

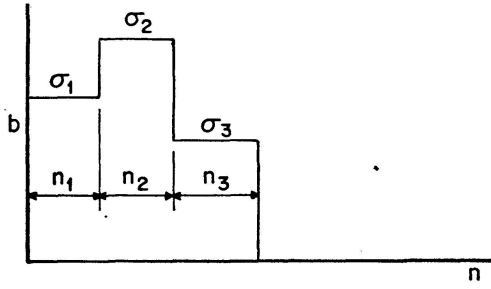


Fig. 2. Stress-Cycle Pattern.

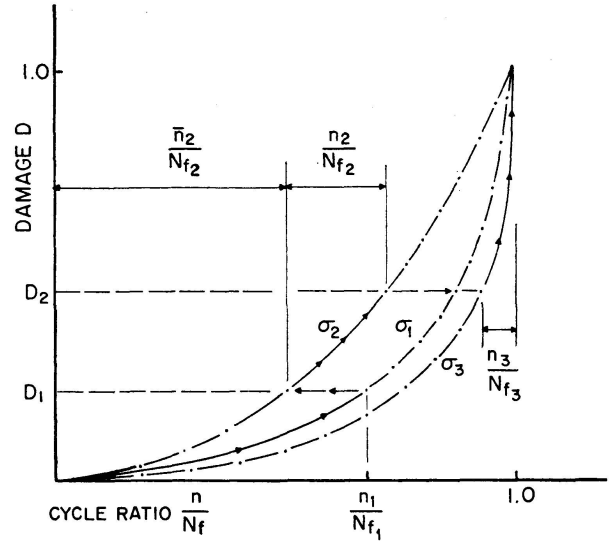


Fig. 3. Damage Accumulation due to Variable Amplitude Loads.

1. Calculate the cycles to failure at the respective stress ranges from Eq. (5) (N_{f1}, N_{f2}, N_{f3}).
2. Evaluate the variable α at the respective stress ranges from Eq. (8) ($\alpha_1, \alpha_2, \alpha_3$).
3. Evaluate damage D_1 due to (n_1) cycles at stress range (σ_1), from Eq. (7).
4. Determine equivalent cycle ratio ($\frac{\bar{n}_2}{N_{f2}}$) producing damage equal to D_1 . Apply Eq. (9), which gives

$$\left(\frac{\bar{n}_2}{N_{f2}}\right) = \left(\frac{n_1}{N_{f1}}\right)^{\alpha_1/\alpha_2}.$$

5. Evaluate the total damage D_2 , due to previous loading (σ_1, n_1) and present loading (σ_2, n_2). Eq. (10) gives:

$$D_2 = D_1 + \Delta D_2 = \left(\frac{\bar{n}_2}{N_{f2}} + \frac{n_2}{N_{f2}}\right)^{\alpha_2}.$$

6. Determine equivalent cycle ratio ($\frac{\bar{n}_3}{N_{f3}}$) providing damage equal to D_2 . Apply Eq. (9), which gives:

$$\left(\frac{\bar{n}_3}{N_{f3}}\right) = \left(\frac{\bar{n}_2}{N_{f2}} + \frac{n_2}{N_{f2}}\right)^{\alpha_2/\alpha_3}.$$

7. The number of cycles (n_3) at stress range (σ_3) that can be sustained up until failure is equal to:

$$n_3 = N_{f3} - \bar{n}_3.$$

The above example demonstrates the application of the proposed equations. These equations can be applied to any pattern of stress levels and any number. A computer program has been written [12] to apply these equations when a large number of stress-cyclic levels are encountered.

Constant Amplitude Tests

Specimen. As shown in Fig. 4, the test specimen was a 12 WF 27 beam with a $5'' \times 3/8'' \times 8'-0''$ welded cover plate, all of ASTM A 36 steel. Strain gages to measure strain accumulation were positioned on top of the bottom flange, at the ends of the cover plates. Additional gages, as shown, were used to monitor load application.

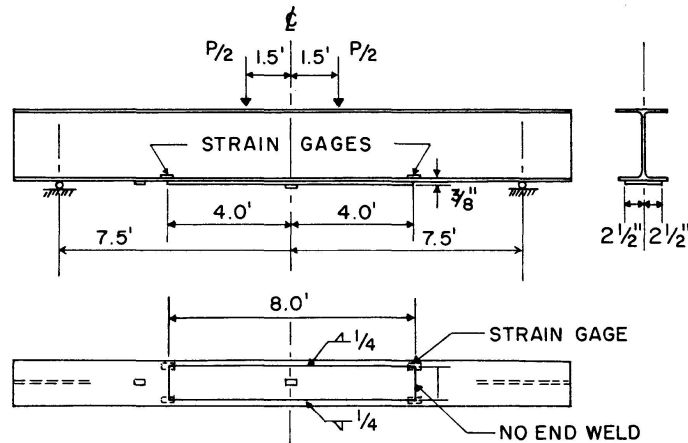


Fig. 4. Test Specimen.

Standard tension tests of coupons taken from the web, flange and cover plate of the test specimens produced an average value of 30.0×10^3 ksi for the Modulus of Elasticity.

Equipment. The fatigue testing equipment consisted of a closed loop hydraulic system with a 20 gpm pump. The accuator has a 50 kip dynamic load capacity.

Ten block programming modules provide the system with the ability to generate a predetermined number of cycles at a certain mean and dynamic amplitude level at various frequencies.

Test Program. As described in Table 1, eleven specimens were tested at constant amplitude. Strain accumulation data was obtained throughout these tests [12].

Test Results. Table 2 describes the constant amplitude test results. Indicated in this table are the cycles to failure of the strain gage which is when the first visible crack appears and when the specimen completely fails or ruptures.

A plot of the cycles to failure, dictated by the gage, and stress range at the cover plate are given in Fig. 5. A least square fit of these data gives:

$$\log N_f = 9.158 - 2.98 \log \sigma_r. \quad (11)$$

This equation is similar to Eq. (5), as was previously described.

In addition to obtaining cycles to failure, strain accumulation data were collected. The data $\left(\frac{d\epsilon}{dn}\right)$ vs. n for specimens CA-1 through CA-9 is given in

Table 1. Constant Amplitude Test Program

| Specimen | Minimum Stress – ksi | | Stress Range – ksi | | Maximum Stress-ksi Centerline |
|----------|----------------------|-------------|--------------------|-------------|-------------------------------|
| | Centerline | End of C.P. | Centerline | End of C.P. | |
| CA-1 | 5.00 | 4.35 | 15.00 | 13.04 | 20.00 |
| CA-2 | 5.00 | 4.35 | 15.00 | 13.04 | 20.00 |
| CA-3 | 5.00 | 4.35 | 15.00 | 13.04 | 20.00 |
| CA-4 | 5.00 | 4.35 | 10.75 | 9.35 | 15.75 |
| CA-5 | 5.00 | 4.35 | 10.75 | 9.35 | 15.75 |
| CA-6 | 5.00 | 4.35 | 20.00 | 17.40 | 25.00 |
| CA-7 | 5.00 | 4.35 | 20.00 | 17.40 | 25.00 |
| CA-8 | 2.00 | 1.75 | 25.00 | 21.75 | 27.00 |
| CA-9 | 2.00 | 1.75 | 25.00 | 21.75 | 27.00 |
| CA-10 | 5.00 | 4.35 | 9.00 | 7.82 | 14.00 |
| CA-11 | 5.00 | 4.35 | 8.00 | 7.00 | 13.00 |

Table 2. Constant Amplitude Test Results

| Specimen Number | Stress Range ksi AT C.P. | Number of Cycles to Failure of Gage | Number of Cycles to Failure of Specimen |
|-----------------|--------------------------|-------------------------------------|---|
| CA-1 | 13.04 | 1,721,500 | 1,907,860 |
| CA-2 | 13.04 | 1,585,200 | 1,787,200 |
| CA-3 | 13.04 | NA | 873,300 |
| CA-4 | 9.35 | 644,500 | 703,700 |
| CA-5 | 9.35 | 518,950 | 582,300 |
| CA-6 | 17.40 | 295,540 | 313,800 |
| CA-7 | 17.40 | 264,600 | 286,800 |
| CA-8 | 21.75 | 138,700 | 151,550 |
| CA-9 | 21.75 | 144,450 | 157,600 |
| CA-10 | 7.82 | 3,109,000* | — |
| CA-11 | 7.00 | 4,100,000* | — |

NA = not operable. * Runout no strain accumulation.

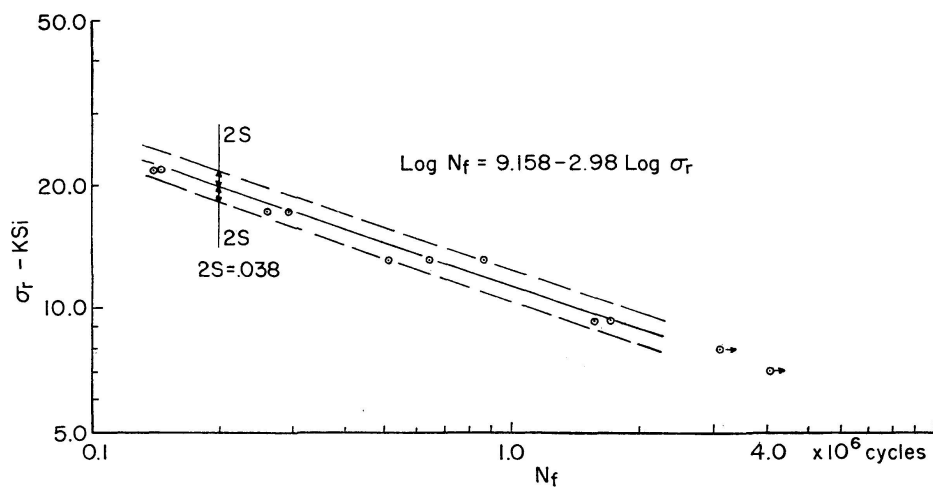


Fig. 5. Stress Range vs. Cycles to Failure.

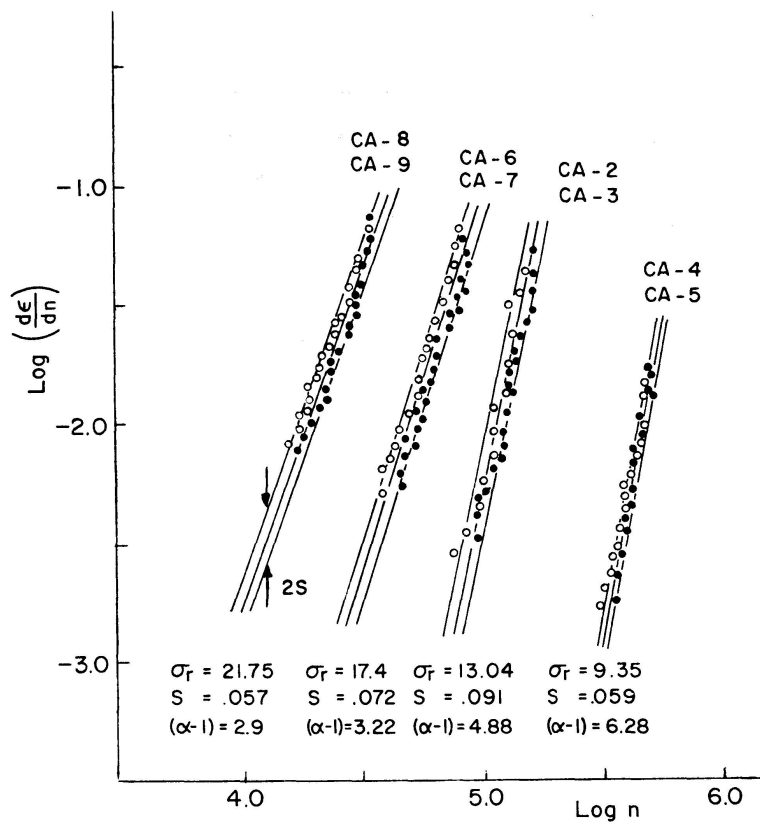


Fig. 6. Strain Accumulation per Cycle vs. Equivalent Number of Cycles.

Fig. 6. A regression line has been established for each specimen, and the respective slope $(\alpha-1)$ determined. A plot of these slopes vs. the stress range σ_r is given in Fig. 7. A least square fit of these data gives the following equation:

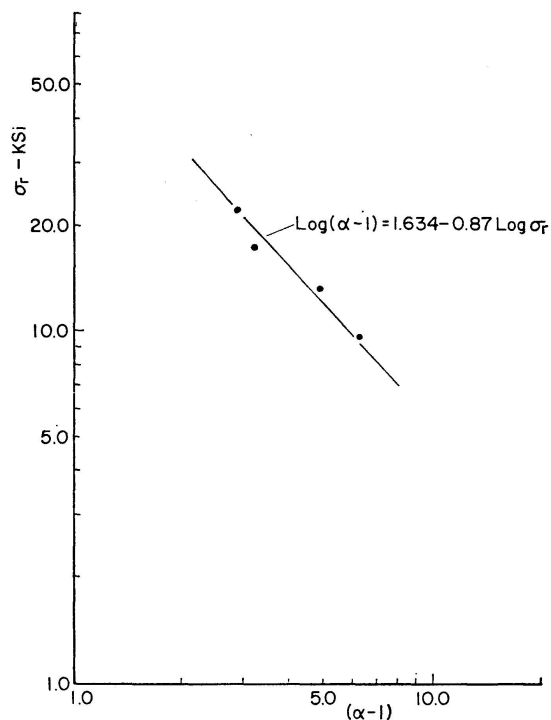


Fig. 7. $(\alpha-1)$ vs. Stress Range.

$$\text{Log}(\alpha - 1) = 1.634 - 0.87 \text{Log} \sigma_r. \quad (12)$$

This equation is similar to Eq. (8), as described previously.

It should be noted that Eq. (11) has been substantiated by the test results obtained at Lehigh University [11]. These tests, however, consisted of some 35 beam specimens and the failure criteria was specimen failure and not gage failure, yielding some slight variations in the $\sigma_r - N_f$ equation.

Variable Amplitude Tests

Test Program. In order to check the validity of the theory, a series of random load tests were conducted. The endurance of the test specimen and strain accumulation was obtained during these tests.

The applied stress and number of cycles, for specimens VAMST 1 through VAMST 4, was selected to represent approximately 20% of the constant amplitude cycles which caused failure. The order of loading consisted of two random, one high to low and one low to high, as described in Fig. 8. The two random loadings, VAMST 1 and 2, consisted of nine block loadings obtained by subdividing the cyclic blocks, given in Fig. 8, except for stress level 13.0 ksi. Specimens VAMST 3 and 4 loadings are as shown in Fig. 8.

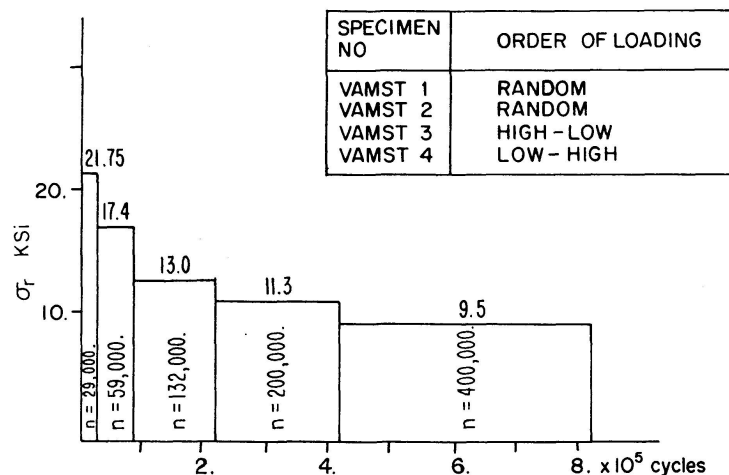


Fig. 8. Variable Amplitude Multi-Step Tests 1-4.

An additional load pattern was selected, Fig. 9, from actual field test data (8). The load factor used was 4.0, as the field data consisted of maximum stress range of 6.0 ksi. The number of consecutively applied cycles, as given by the field data, was also increased 300 times, to examine the effects of a large number of consecutive cycles. Additional tests of this type have also been conducted [12], and yield similar results, now to be presented.

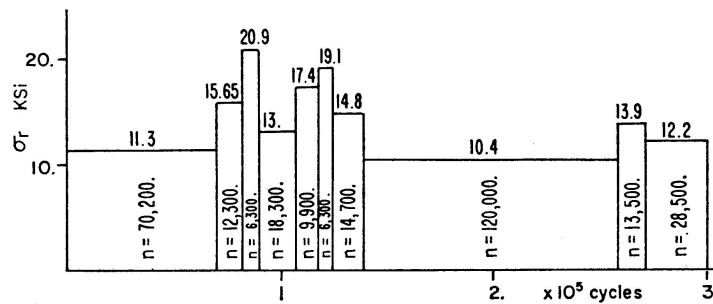


Fig. 9. Variable Amplitude Multi-Step Test 5.

Test Results. As described in Fig. 8, the cover plated specimens were subjected to five varying stress levels at a specific number of cycles per level. The first two specimens, VAMST 1 and VAMST 2, were subjected to a random set of these stress range levels. The random pattern selected resulted in the following order of stress range levels: $\sigma_r = 9.5, 21.75, 17.4, 11.3, 13.0, 11.3, 9.5, 17.4, 21.75, 9.5$. Specimen VAMST 1, had gage failure in the ninth block at a stress range level of 21.75 ksi. Specimen VAMST 2, gage failed in the tenth block at stress range level of 9.5 ksi. The total number of cycles at failure are given in Table 3.

Table 3. Variable Amplitude Multi-Step Test Results

| Specimen Number | Number of Cycles at Failure of Gage | Number of Cycles at Failure of Specimen | Stress Range at Failure of Gage - ksi | Number of Blocks at Gage Failure |
|-----------------|-------------------------------------|---|---------------------------------------|----------------------------------|
| VAMST 1 | 819,500 | 980,000 | 21.75 | 9 |
| 2 | 889,500 | 1,023,000 | 9.50 | 10 |
| 3 | 650,000 | 825,400 | 9.50 | 5 |
| 4 | 1,451,000 | 1,516,000 | 13.00 | 8 |
| 5 | 866,500 | 978,205 | 13.90 | 29 |

Specimen VAMST 3, was subjected to a high to low stress level of loading. This specimen failed after application of the fifth stress level ($\sigma_r = 9.5$ ksi) or fifth block, as listed in Table 3.

Specimen VAMST 4, which was subjected to a low to high stress pattern as given in Fig. 8, had failure of the gage during the eighth block loading ($\sigma_r = 13.0$ ksi). This specimen was, therefore, subjected to one complete loading pattern (5 blocks), with initiation of 3/5 of a similar pattern. Table 3, describes the accumulative number of cycles absorbed by this specimen. The order of loading and resulting cycles to failure is most apparent in comparing this data with specimen VAMST 3 data.

Specimen VAMST 5, which was subjected to stress levels and cyclic variations representing actual field data had gage failure after 29 block loadings. The stress level at gage fail was 13.9 ksi, as listed in Table 3.

Comparison with Theory. A comparison between the experimental data and the proposed theory and theories by MINER [13] and HENRY [14], are given in Table 4. The predicted number of cycles to failure, according to the three theories, shows that all three theories are conservative. A comparison between block ratios, n/N_f , at the failure block are also listed.

Table 4. Comparison of VAMST Results with Theory

| Spec. No. | Acc. No. of Cycles to Fall | Stress Level at Failure of Gage ksi | Calculated Cum. No. of Cycles | | | Failure Block Ratio | |
|-----------|----------------------------|-------------------------------------|-------------------------------|--------|--------|----------------------|---------------|
| | | | Theory | Miner | Henry | Theory \bar{n}/N_f | Miner n/N_f |
| VAMST 1 | 819000 | 21.75 | 809100 | 775000 | 672500 | 1.01 | 1.01 |
| 2 | 889000 | 9.5 | 809100 | 775000 | 672500 | 1.05 | 1.05 |
| 3 | 650000 | 9.5 | 450000 | 816600 | 615000 | 1.10 | 0.91 |
| 4 | 1451000 | 13.0 | 980000 | 816600 | 898000 | 1.14 | 1.52 |
| 5 | 866500 | 15.9 | 701000 | 709300 | 660000 | 1.13 | 1.16 |

N_f = number of constant amplitude cycles at last stress level to cause failure.

\bar{n} = calculated number of cycles at last stress level to induce final failure damage.

n = given number of cycles at calculated stress failure level.

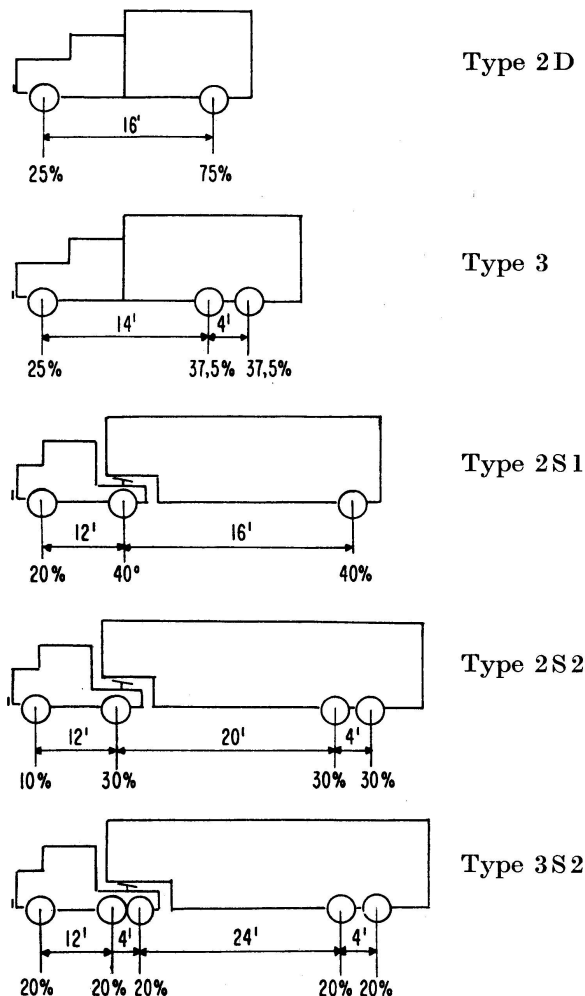


Fig. 10. Truck Types.

Application

Truck Classifications. Examination of extensive field data [5], [6], [7], [8] has resulted in five typical truck types, as given in Fig. 10. The distribution of axle weight and axle spacings are typical for the present traffic trends.

Maximum Moments. The maximum moments induced in a simply supported beam, due to these moving loads, have been calculated assuming gross weight equal to 72.0 kips and span lengths ranging from 10 to 100 feet. These maximum moments can be related to stress range and the property (Z/L) , section modulus divided by span length. A relationship between N_f , α and (Z/L) is then obtained by applying Eqs. (11) and (12), which give for span length ranges:

$$0 \leq L \leq 40',$$

$$\text{Log } N_f = 9.158 - 2.98 \text{Log} \left(\frac{K_1}{Z/L} \right), \quad (13)$$

$$\text{Log} (\alpha - 1) = 1.634 - 0.87 \text{Log} \left(\frac{K_1}{Z/L} \right), \quad (14)$$

$$40' \leq L \leq 100',$$

$$\text{Log } N_f = 9.158 - 2.98 \text{Log} \left(\frac{\bar{K}}{Z/L} \right), \quad (15)$$

$$\text{Log} (\alpha - 1) = 1.634 - 0.87 \text{Log} \left(\frac{\bar{K}}{Z/L} \right), \quad (16)$$

where K_1 and \bar{K} are constants as established for the given truck types. A plot of Eqs. (13) through (16), considering upper and lower bounds on \bar{K} , yields

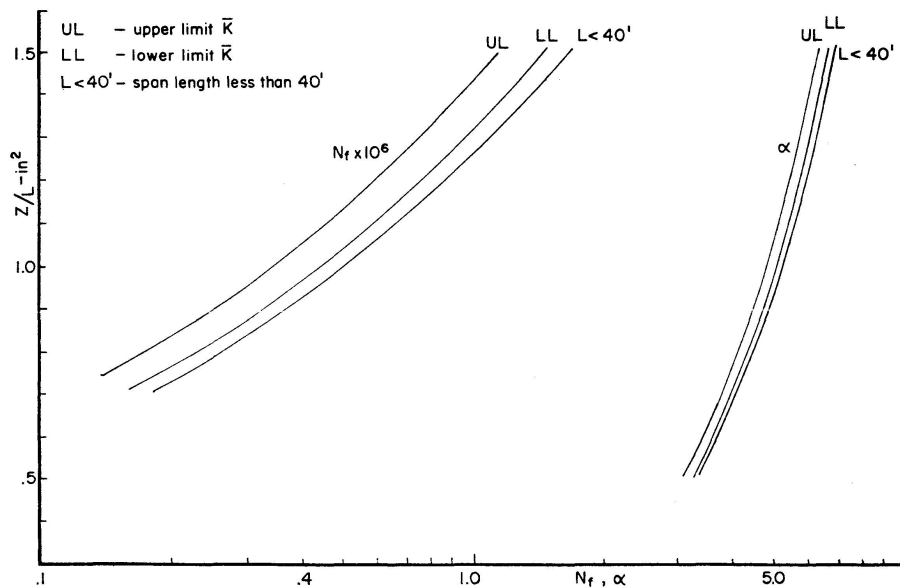
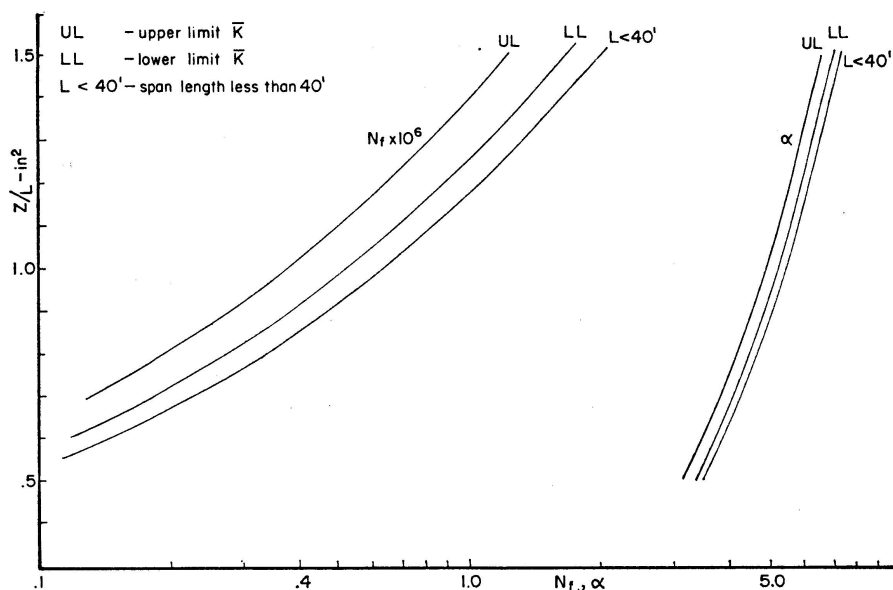
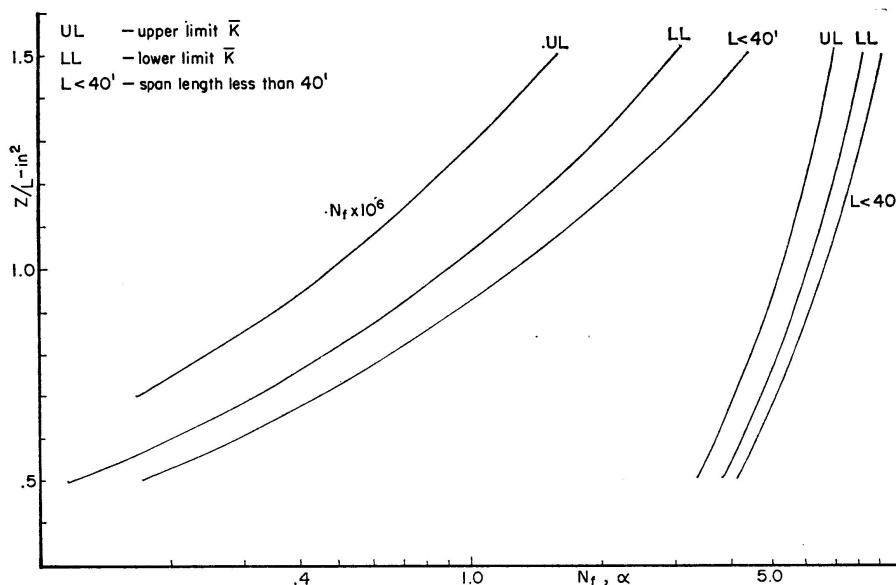
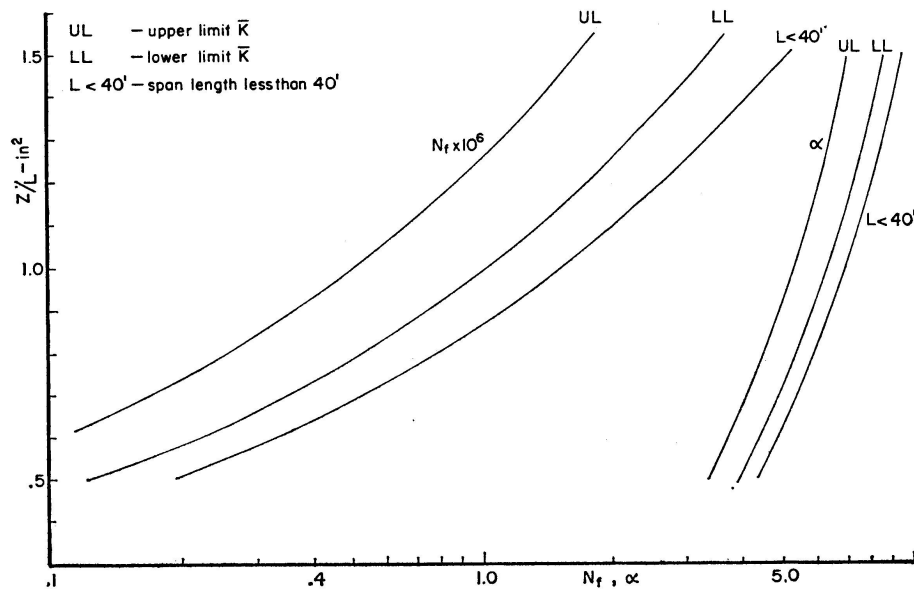
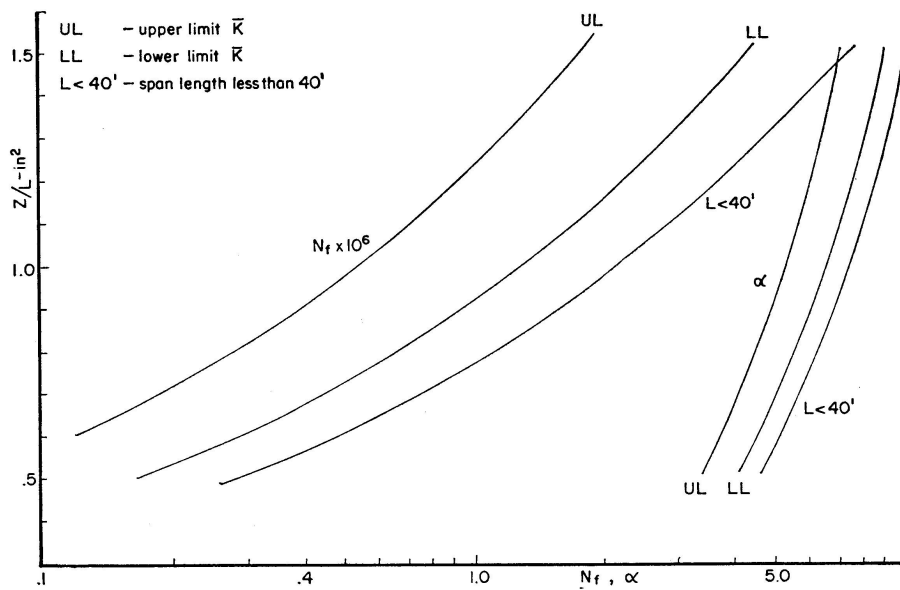


Fig. 11. N_f, α Curves for 2 D Truck Type.

Fig. 12. N_f, α Curves for 3 Truck Type.Fig. 13. N_f, α Curves for 2 S-1 Truck Type.

Figs. 11 through 15. These curves can then be applied in conjunction with particular load patterns, as described previously.

It should be noted that all of these curves are for vehicles whose gross weight equals 72.0 kips. The values obtained from these curves or Eqs. (13) and (14) should be multiplied by the factor $(72/GW/DF)^{2.98}$ and Eqs. (15) and (16) by the factor $(72/GW/DF)^{0.87}$, for other gross weights where (GW) represents the gross weight and (DF) equals the distribution factor.

Fig. 14. N_f, α Curves for 2 S-2 Truck Type.Fig. 15. N_f, α Curves for 3 S-2 Truck Type.

Notations

- A a stress dependent material constant
- b intercept of $\text{Log } \sigma_r$ vs. $\text{Log } N_f$ equation
- c slope of $\text{Log } \sigma_r$ vs. $\text{Log } N_f$ equation
- d intercept of $\text{Log } (\alpha - 1)$ vs. $\text{Log } \sigma_r$ equation
- e slope of $\text{Log } (\alpha - 1)$ vs. $\text{Log } \sigma_r$ equation
- D damage
- D_i damage due to n_i cycles

| | |
|------------------------|--|
| K, K_1 | constants |
| N_f | number of constant amplitude cycles to failure |
| n | number of consecutive cycles |
| \bar{n} | equivalent number of cycles |
| n/N_f | cycle ratio |
| \bar{n}/N_f | equivalent cycle ratio |
| S | standard deviation |
| α | a stress dependent material constant |
| ϵ_p, ϵ | accumulated plastic strain at n cycles |
| ϵ_f | accumulated strain at failure |
| $d\epsilon_p/dn$ | accumulated strain per cycle |
| γ | a stress dependent material constant |
| σ_r | stress range at cover plate end, except as noted |

Acknowledgements

The analytical and experimental studies contained herein are part of a research project sponsored by the Maryland State Roads Commission and the U.S. Bureau of Public Roads. Their guidance and help is gratefully acknowledged.

Bibliography

1. "Loading Histories of Highway Bridges, Program to Gather Field Data." Information from Structures and Applied Mechanics Division, Office of Research and Development, U.S. Bureau of Public Roads, March 1, 1968.
2. Highway Research Circular # 61, Highway Research Board, Research Problem # 76, # 60, January 1967.
3. "A Strain History Data System for Use on Highway Bridges." C. F. Galambos, BPR Washington, D.C., HRB January 1967.
4. "Loading History of Highway Bridges." C. F. Galambos, W. L. Armstrong, BPR Washington, D.C., HRB January 1969.
5. "Induced Dynamic Strains in Bridge Structures due to Random Truck Loadings." M. W. Novak, C. P. Heins, C. T. G. Looney, Civil Engineering Dept., University of Maryland, College Park, Md., Feb. 1968, Rept. No. 18.
6. "Tabulation of 24 Hour Dynamic Strain Data on Four Simple Span Girder-Slab Bridge Structures." C. P. Heins, Jr., Arthur D. Sartwell, Civil Engineering Dept., University of Maryland, College Park, Md., June 1969, Rept. No. 29.
7. Tabulation of Dynamic Strain Data on a Three Span Continuous Bridge Structure." A. D. Sartwell, C. P. Heins, Jr., Civil Engineering Dept., University of Maryland, College Park, Md., Nov. 1969, Rept. No. 33.
8. "Tabulation of Dynamic Strain Data on a Girder-Slab Bridge Structure During Seven Continuous Days." A. D. Sartwell, C. P. Heins, Jr., Civil Engineering Dept., University of Maryland, College Park, Md., Sept. 1969, Rept. No. 31.
9. "Elastic Hysteresis Property of Several Steels under Fatigue Load." Kawamoto, M., Tanaka, T., Trans. Japan Society of Mechanical Engineers, 1965.

10. "Processes of Creep and Fatigue in Metals." A. J. Kennedy, John Wiley, N. Y., 1963.
11. "Effect of Weldments on Fatigue Strength of Steel Beams." J. W. Fisher et al., Lehigh Univ., Bethlehem, Pa., Sept. 1969, Fritz Lab. Rept. No. 334.2.
12. "Fatigue of Beams with Welded Cover Plates." F. A. Murad, C. P. Heins, Civil Engineering Dept., University of Maryland, College Park, Md., Sept. 1970, Rept. No. 38.
13. "Cumulative Damage in Fatigue." M. A. Miner, J. Appl. Mech. Vol. 12, No. 1, Sept., 1945.
14. "A Theory of Fatigue-Damage Accumulation in Steel." D. L. Henry, Trans. ASME, Vol. 77, No. 6, Aug. 1955.

Summary

The fatigue life of steel beams with welded cover plates is predicted by a strain accumulation damage theory. The theory permits application of random loads, thus considers load order. The resulting equations are applied to the response of five typical truck types on a simple span of varying lengths.

Résumé

La résistance à la fatigue de poutres en acier avec des couvre-joints soudés est déterminée à l'avance grâce à la théorie des déformations et des détériorations. La théorie permet l'application de charges supplémentaires et tient compte de leur ordre de grandeur. Les équations qui en résultent sont alors appliquées au comportement de cinq types de véhicules sur une ouverture simple de portée variable.

Zusammenfassung

Die Ermüdungsdauer von Stahlträgern mit geschweissten Deckplatten wird mittels einer Verformungs-Schadentheorie vorausbestimmt. Die Theorie gestattet die Anwendung von Zusatzbelastungen und zieht so die Grösse der Belastung in Betracht. Die sich ergebenden Gleichungen werden auf das Verhalten von fünf Typen von Fahrzeugen auf einfache Öffnungen variabler Länge angewandt.

Leere Seite
Blank page
Page vide